

# **Turbulence and transport in the edge region of toroidally magnetized plasmas**

**O. E. Garcia, V. Naulin, A. H. Nielsen, and J. Juul Rasmussen**

*Association EURATOM-Risø National Laboratory,*

*Technical University of Denmark, OPL-128,*

*P.O. Box 48, DK-4000 Roskilde, Denmark*

## **Abstract**

Intermittent transport of particles and heat in the boundary region of toroidally magnetized plasmas is investigated by means of two-dimensional fluid turbulence simulations. The model describes the non-linear dynamics of interchange modes, coupling a plasma edge region with localized sources of particles and heat to an effective scrape-off layer with linear damping of the dependent variables due to transport along open magnetic field lines. An intermittent turbulent state is maintained by a steep pressure profile in the edge region. The turbulence spreads out through the scrape-off layer in a bursty manner in the form of blob structures. The rescaled probability distribution functions of the local particle density fluctuations as well as the turbulent radial particle flux at different radial positions in the scrape-off layer fall into coincidence, thus indicating universality of the fluctuation and transport statistics. Coarse graining further reveals that the particle density fluctuations possess a range of self-similarity and long range correlations on time scales from the correlation time to that of the bursting in the turbulence intensity.

Mixing and spreading of impurities in the scrape-off layer by the intermittent turbulence is investigated by means of the test particle approach. The particle dynamics is dominated by long flights and cannot be described by diffusive processes. However, the impurities are found to mix effectively throughout the scrape-off-layer on short time scales covering only a few global bursts periods. The impurities undergo a pinch-like transport mitigated by the compressibility of the electric drift due to the inhomogeneous magnetic field.

## I. INTRODUCTION

A characteristic feature of turbulent flows is the ability to transport and mix particles and heat. This process is rather complicated even under idealized conditions of homogeneous and isotropic turbulence and is still far from being understood in general. Covering a variety of important areas from the diffusion of pollutants in environmental flows to the particle and heat diffusion in magnetized plasmas in fusion devices this topic connects basic research with applications.

In magnetized plasmas it is now well established that the enhanced levels of cross-field energy and charged particle transport observed in a wide variety of devices, including tokamaks and stellarators, is mainly due to low-frequency, electrostatic, micro-turbulence, with the  $E \times B$ -drift as the dominating velocity, in particular in the edge region (see, e.g., Refs. 1 and 2). This transport is usually termed anomalous transport<sup>3</sup> and is far dominating the classical collisional transport. Even if the turbulence and the transport characteristics observed in various experiments show similar behaviors a detailed understanding of the underlying mechanisms driving the fluctuations and the associated transport is still not at hand.

It is worthwhile to mention here, that in plasmas there are two ways to determine the charged particle transport properties of a turbulent flow-field. One is to look directly at the convected density, leading to an expression  $\vec{\Gamma} = \tilde{n} \vec{v}_{E \times B}$  for the local density flux, where  $\tilde{n}$  and  $\vec{v}_{E \times B}$  are the density fluctuations and the  $E \times B$  velocity, respectively. This is the cross-field transport as usually measured in experiments and simulations of electrostatic turbulence, e.g., [4–6], it includes the transport of mass. The other way, is to investigate the dispersion of passive test particles, which are traced over time, and thereby to determine a diffusion coefficient. The flux is then obtained via Fick's law. This approach originates from the original studies in classical fluid turbulence dating back to the works of Taylor<sup>7</sup> (see, e.g., Ref. 8). In the context of plasma turbulence this approach has been pioneered by Balescu and co-workers in several contributions (cf. Ref. 3) including the connection between the Lagrangian and Eulerian statistics, e.g., Ref. 9, the scaling of the diffusion coefficient with the RMS value of the fluctuations, e.g., Refs. 10 and 11, and the magnetic field strength, e.g., Ref. 12.

The relation between the test particle diffusion and the plasma transport, i.e., the particle density flux, across the magnetic field is not straightforward. The flux is degrading the the plasma confinement and acts back on the turbulence, while the test particle diffusion rather reflects the mixing properties of the turbulent flow and one has to rely on Fick's law to provide direct infor-

mation on the cross-field transport, i.e., the flux  $\Gamma = -D\nabla n$ , where  $D$  is the diffusion coefficient of the passive tracers. However, the direct relationship has indeed indeed demonstrated for the case of 2D drift wave turbulence.<sup>13,14</sup> Furthermore, it should be mentioned that the dynamics of test particles has also been investigated in connection with the transport of impurities in the plasma, see, e.g., Refs. 15–17. In particular, it was demonstrated that heavier impurities have a tendency to cluster in vortical structures.<sup>16</sup>

In the following, we shall concentrate the discussion on the turbulence and transport in the edge region and scrape-off-layer, SOL, of a magnetized plasma. It is well established that the cross field transport of particles and heat near the boundary of magnetically confined plasmas is strongly intermittent. This is observed in a variety of devices including linear<sup>4,18,19</sup> as well as toroidal configurations.<sup>19–22</sup> Detailed investigations have revealed strong indications that the intermittent nature of particle and heat transport is caused by localized structures in the form of field-aligned filaments or blobs propagating radially far into the SOL of magnetized plasmas.<sup>18–22</sup> It has been suggested that the radial propagation is caused by a dipolar vorticity field formed by the charge separation in a blob of plasma due to guiding-center drifts in a non-uniform magnetic field.<sup>23</sup> This simple model provides the qualitative features of radial plasma blob propagation, for a more detailed discussion of the blob dynamics we refer to Garcia *et al.*<sup>24</sup> However, a model describing both the formation and dynamical evolution of such structures in a self-consistent way has remained elusive.

The blob structures are elongated along the magnetic field but have a finite parallel correlation length due to the ballooning effect imposed by the toroidal geometry. Thus, the structures in the edge and SOL take the form of long “sausages” winding around the plasma by following the flux tubes of the ambient magnetic field, similar to the recent visualization of field-aligned structures in a spherical tokamak device,<sup>25</sup> which were ascribed to edge localized modes (ELM s). In the SOL the structures gradually decay in amplitude due to transport along open field lines. Recent investigations, for example those given in Ref. 26, have shown that the fine structure and radial propagation of ELM s through the SOL have striking similarities with the nonlinear blob structures, although standard ELM theories are based on a combination of the MHD ballooning and peeling instabilities, see, e.g., Fundamenskii *et al.*<sup>27</sup>

In this contribution we present a brief overview of recent results obtained from a self-consistent description of the intermittent particle and heat transport demonstrating the emergence and evolution of such blob-like structures in the edge/SOL region of a toroidally magnetized plasma.<sup>28–30</sup> The investigations are based on the so-called ESEL (Edge-Sol-ELectrostatic)

model for interchange turbulence in local slab geometry at the outboard mid-plane of the toroidal plasma. The model includes the self-consistent evolution of the full thermodynamic and flow profiles. The geometry comprises distinct production and loss regions, corresponding to the edge and SOL of magnetized plasmas. The separation of these two regions defines an effective last closed flux surface (LCFS). In the edge region, where the sources of particles and heat are located, strong pressure gradients maintain a state of turbulent convection. The driving instability is the interchange mode due to an inhomogeneous magnetic field. We ignore the parallel electric currents as well as magnetic shear and restrict ourself to electrostatic perturbations. On the other hand, we retain the full nonlinear structure of the flow compression terms, which are mandatory in order to describe the order unity perturbations to the ambient plasma parameters. The three-dimensional structure of the blobs is accounted for by simple linear damping terms in an effective SOL region. A self-regulation mechanism involving differential rotation leads to repetitive expulsions of hot plasma into the SOL, resulting in a strongly intermittent transport of particles and heat.

We shall particularly discuss the basic statistical properties of the particle density fluctuations as well as the radial turbulent particle flux in the SOL region. We observe highly skewed probability density functions (PDF s) with pronounced exponential tails toward large fluctuations, consistent with radial transport by blob structures. There are indications of long-range correlations with a self-similar scaling of the PDF s for increasingly coarse grained particle density signals in the SOL, at least up to the time scale of the bursting in the global turbulence intensity.

Additionally, we have investigated the mixing and spreading of impurities in the scrape-off layer by the intermittent turbulence by means of the test particle approach. The particle dynamics is found to be dominated by long flights in radially outgoing as well as radially ingoing directions and cannot be described by diffusive processes. Particles released locally either in the far SOL or near the LCFS are found to be mixed effectively over the full domain within a time corresponding to only a few burst periods. The impurities undergo a pinch-like transport mitigated by the compressibility of the electric drift due to the inhomogeneous magnetic field.

The results from the ESEL code have been compared with experimental observations of turbulence and transport in the edge/SOL of toroidal devices and generally found to in close agreement with these observations. Particular mention should be made of the the direct detailed comparisons with the the results from the TCV-tokamak at CRPP, EPFL in Lausanne.<sup>31-34</sup> This showed the first ever quantitative agreement between experimental data and numerical results

from a first-principle based numerical modeling both with respect to the profiles of density and temperature in the SOL, the fluctuations and the associated transport. These detailed comparisons are facilitated by applying realistic collision operators calculated with the measured density and temperature.<sup>35</sup> Thus, the input parameters to the code are basically the temperature and density measured at last closed flux surface LCFS. Similar detailed comparisons have been initiated for other devices as well, including JET,<sup>35,36</sup> with very promising results.

These results provide great confidence that SOL turbulence is largely governed by interchange motions, and opens up possibilities for eventual predictive capability for SOL transport levels.

This paper is organized as follows. The model equations are briefly described in Sec. II. In Sec. III we first discuss the global energy evolution and the spatial structure of the particle density. A detailed statistical analysis is then given of the particle density fluctuations and the turbulent flux recorded at different radial positions covering the edge and the SOL regions. In Sec. IV we describe the radial spreading and mixing of impurities, modeled as passive tracers, in the SOL. The final section V contains our concluding remarks.

## II. MODEL EQUATIONS FOR THE DYNAMICS IN THE EDGE/SOL

The model is based on the fluid equations assuming low-frequency electrostatic fluctuations. They are derived from the continuity equation for the electrons, the electron temperature equation and the quasi-neutrality condition. Assuming cold ions and neglecting electron inertia effects, we obtain a three-field model for the evolution of the full particle density  $n$ , electric potential  $\phi$  and electron temperature  $T$ . Using local slab coordinates with  $\hat{z}$  along the magnetic field,  $\hat{x}$  in the radial and  $\hat{y}$  in the poloidal direction the equations may be written as<sup>28–30</sup>

$$\frac{d\Omega}{dt} - C(p) = \nu_{\Omega} \nabla^2 \Omega - \sigma_{\Omega} \Omega, \quad (1a)$$

$$\frac{dn}{dt} + nC(\phi) - C(nT) = \nu_n \nabla^2 n - \sigma_n (n - 1) + S_n, \quad (1b)$$

$$\frac{dT}{dt} + \frac{2T}{3} C(\phi) - \frac{7T}{3} C(T) - \frac{2T^2}{3n} C(n) = \nu_T \nabla^2 T - \sigma_T (T - 1) + S_T, \quad (1c)$$

where the vorticity is given by  $\Omega = \nabla_{\perp}^2 \phi$ . Time is normalized by  $1/\omega_{ci}$  and spatial scales by  $\rho_s = c_s/\omega_{ci}$ , where  $\omega_{ci}$  is the ion cyclotron frequency and  $c_s$  is the acoustic speed. The particle density  $n$  and temperature  $T$  are normalized to fixed characteristic values at the outer wall. We further define the advective derivative, the magnetic field curvature operator and the toroidal

magnetic field by

$$\frac{d}{dt} = \frac{\partial}{\partial t} + \frac{1}{B} \hat{\mathbf{z}} \times \nabla \phi \cdot \nabla, \quad C = -\zeta \frac{\partial}{\partial y}, \quad B = \frac{1}{1 + \varepsilon + \zeta x}. \quad (2)$$

with the inverse aspect ratio  $\varepsilon = a/R_0$  and  $\zeta = \rho_s/R_0$ , where  $a$  and  $R_0$  are the minor and major radius of the device, respectively. The terms on the right hand side of the equations describe external sources  $S$ , parallel losses along open field lines through the damping rates  $\sigma$ , and collisional diffusion with coefficients  $\nu$ . The geometry and boundary conditions are sketched in Fig. 1. Further discussions of the model may be found in Ref. 35, with particular attention to the collision operators and parallel loss terms. A local linear stability analysis for fluctuations around a fixed gradient yields the well-known characteristics of the ideal interchange instability.<sup>37,38</sup>

In order to describe the global evolution of the convective system we introduce kinetic energy integrals of the fluctuating motions and the poloidally mean flow component  $v_0$ ,

$$K = \int d\mathbf{x} \frac{1}{2} \left( \nabla_{\perp} \tilde{\phi} \right)^2, \quad U = \int d\mathbf{x} \frac{1}{2} v_0^2, \quad (3)$$

where the zero index denotes an average over the poloidal direction and the spatial fluctuation about this mean is indicated by a tilde. The evolution of these energy integrals is found by multiplying the vorticity equation (1a) by the electrostatic potential and integrating over the plasma layer under consideration,

$$\frac{dK}{dt} = \zeta \int d\mathbf{x} n T \tilde{v}_x + \int d\mathbf{x} v_0 \frac{\partial}{\partial x} (\tilde{v}_x \tilde{v}_y)_0 - \int d\mathbf{x} \tilde{\phi} \Lambda_{\Omega}, \quad (4a)$$

$$\frac{dU}{dt} = - \int d\mathbf{x} v_0 \frac{\partial}{\partial x} (\tilde{v}_x \tilde{v}_y)_0 - \int d\mathbf{x} \phi_0 \Lambda_{\Omega}. \quad (4b)$$

where  $\Lambda_{\Omega} = \nu_{\Omega} \nabla^2 \Omega - \sigma_{\Omega} \Omega$ . The mean flow  $v_0 = \partial \phi_0 / \partial x$ , corresponding to differential rotation, does not yield any radial transport of particles and heat and hence form a benign path for fluctuation kinetic energy. The first term on the right hand side of Eq. (4) describes the drive of fluctuating motions due to radially outwards transport of thermal energy, while the second term reveals the conservative transfer of kinetic energy from the fluctuating motions to the sheared flows in Eq. (4b). The last term in both equations describes linear damping due to collisional diffusion and parallel losses. Some recent discussions on convective turbulence with self-sustained sheared flows may be found in Refs. 38 and 39.

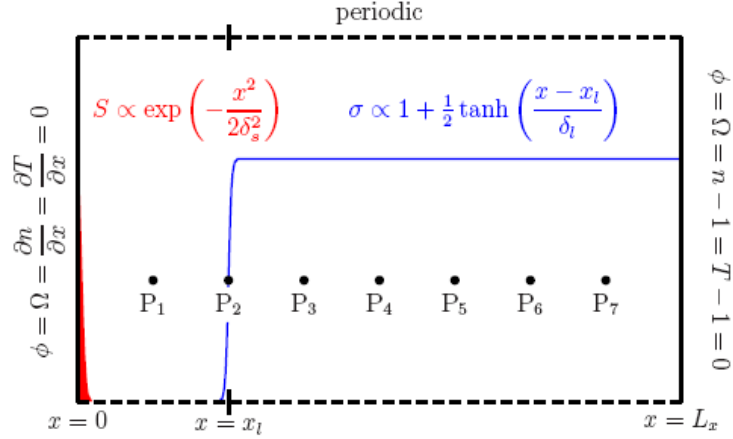


FIG. 1: Geometry of the simulation domain showing the forcing region to the left, corresponding to the edge plasma, and the parallel loss region to the right, corresponding to the scrape-off layer. Data time series are collected at the seven probes  $P_i$ .

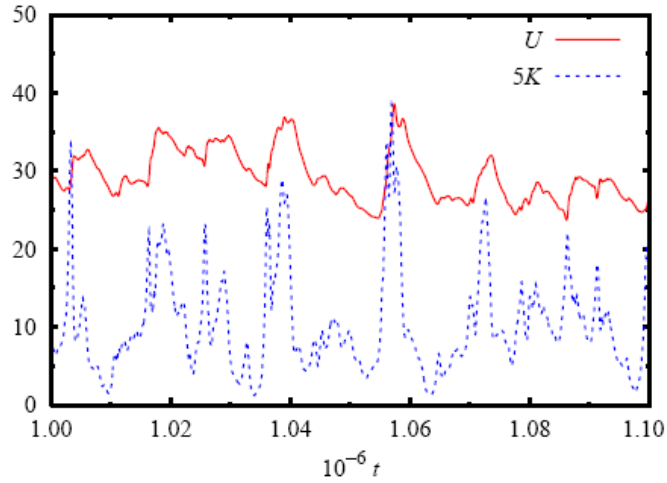


FIG. 2: Evolution of the kinetic energy contained in the fluctuating motions,  $K$ , and the poloidally mean flows,  $U$ .

### III. TURBULENCE AND INTERMITTENT TRANSPORT IN THE SOL

In the following we discuss the basic results obtained with the ESEL-code using parameters relevant for SOL plasmas, for details see Ref. 28–30. We take  $L_x = 2L_y = 200$  with the LCFS located at  $x_l = 50$ , confer Fig. 1. The parameters are  $\delta_s = \sqrt{2}$ ,  $\delta_l = 1$ ,  $\varepsilon = 0.25$ ,  $\zeta = 5 \times 10^{-4}$ , and  $\nu = 10^{-2}$  for all fields.

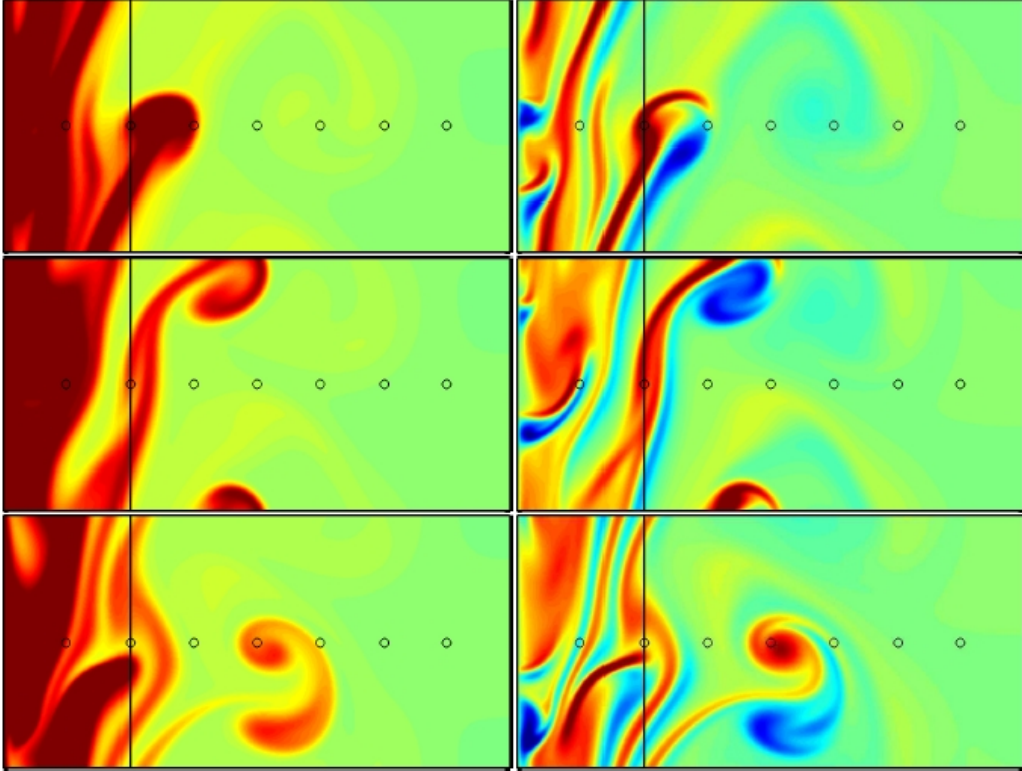


FIG. 3: Evolution of the particle density to the left and the electric drift vorticity to the right during one global turbulence burst at times  $t = 1071250$  (top row),  $t = 1071750$  (middle row), and  $t = 1072250$  (bottom row).

The parallel loss rate of temperature is assumed to be five times larger than that on the particle density and vorticity,  $\sigma_n = \sigma_\Omega = \sigma_T/5 = 3\zeta/4\pi q$ , since primarily hot electrons are lost by parallel transport. The damping rates  $\sigma_n$  and  $\sigma_\Omega$  correspond to losses to the nearest target plate over a parallel distance of  $L_{||} = 2\pi q R_0/3$  with half the acoustic velocity, where  $q = 7.5$  is the safety factor in the SOL. Finally, the radial line-integral of the sources  $S_n$  and  $S_T$  equals  $10^{-3}$ . For the numerical solution a spatial resolution of  $512 \times 256$  grid points in the radial and poloidal directions is used, and we follow the evolution of the statistically stationary turbulence for more than  $10^6$  time units. This temporal range covers all the relevant time scales of the problem, from the fast interchange time scale to several hundred diffusive time scales. The chosen parameter values serve to illustrate a robust nonlinear dynamics observed for a large range of parameters.

The numerical simulations reveal a state of large-scale intermittency in which quiet periods are interrupted by strong bursts of turbulent activity accompanied by radially outwards particle

and heat transport. This behavior is evident from Fig. 2, where we present the evolution of the energy components defined in Eq. (3). The energy  $U$  in the mean poloidal flow is found to be significantly larger than the energy  $K$  in the fluctuating motions. The latter component shows pronounced bursts which terminate by a rapid transfer of kinetic energy to the mean flow, described by Eqs. (4). The mean flow controls the dynamics during the quiet phases, where it is damped on a slow viscous time scale resulting in quasi-periodic relaxation oscillations. This global self-regulating dynamics is typical for two-dimensional convective turbulence.<sup>38–40</sup>

The spatial structure of the particle density and the electric drift vorticity is depicted in Fig. 3 during one turbulence intensity burst shown in Fig. 2. The turbulence is maintained by the unstable interchange modes in the edge region where a steep pressure profile resides, and spreads into the linearly stable SOL region where the pressure profile is nearly flat. The particle density in the SOL takes the form of a localized blob that is formed inside the LCFS and propagate outwards through the SOL with a decaying amplitude due to losses along the open magnetic field lines. Associated with the blob structure in the particle density is a dipolar electrostatic potential and vorticity field consistent with a vertical charge polarization due to magnetic guiding center drifts.

From correlation analysis and conditional averaging we find that the radial propagation velocity of the blob structures corresponds to around  $0.05c_s$ , with a significant statistical variance, in agreement with experimental measurements.<sup>18–21</sup>

A detailed analysis of the propagation dynamics of individual blob structures is performed by Garcia *et al.*<sup>24</sup> This includes a scaling of the blob velocity with blob size and various plasma parameters:  $v_b/c_s = (2\ell\Delta p/R_0p_0)^{1/2}$ , where  $\ell$  is the size of the structure in the plane perpendicular to the magnetic field,  $\Delta p/p_0$  is the relative amplitude of the blob structure. For typical parameters this provides a velocity of  $v_b/c_s \leq 0.1$ . In addition the influence of various dissipation mechanisms are considered, including the sheath dissipation which comes into play when blobs are connected to the divertor plates.

Statistical analysis of signals from single-point recordings at different radial probes  $P_i$  as indicated in Fig. 1 agree generally very well with experimental measurements.<sup>28–30</sup> Here we concentrate on the statistical properties of the particle density fluctuations and the associated turbulent transport. Figure 4a shows the radial variation of the skewness factor  $S$  and the flatness factor  $F$  for the particle density fluctuations (both  $S$  and  $F$  vanish for a normal distribution). As found from the experimental measurements, the particle density fluctuations just inside the LCFS are normally distributed, while the skewness and flatness increases outwards in the SOL.

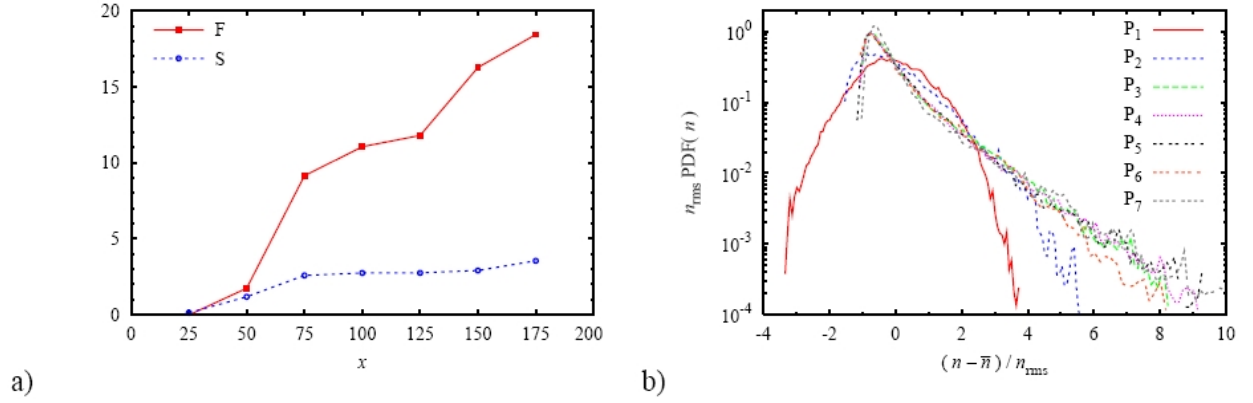


FIG. 4: a) Radial variation of the flatness,  $F$ , and the skewness,  $S$ , of the local particle density fluctuations (left panel). b) Rescaled PDF s of particle density fluctuations measured by the seven probes  $P_i$  shown in Fig. 1. The averaged particle density and standard deviation are designated by  $\bar{n}$  and  $n_{\text{rms}}$ , respectively (right panel).

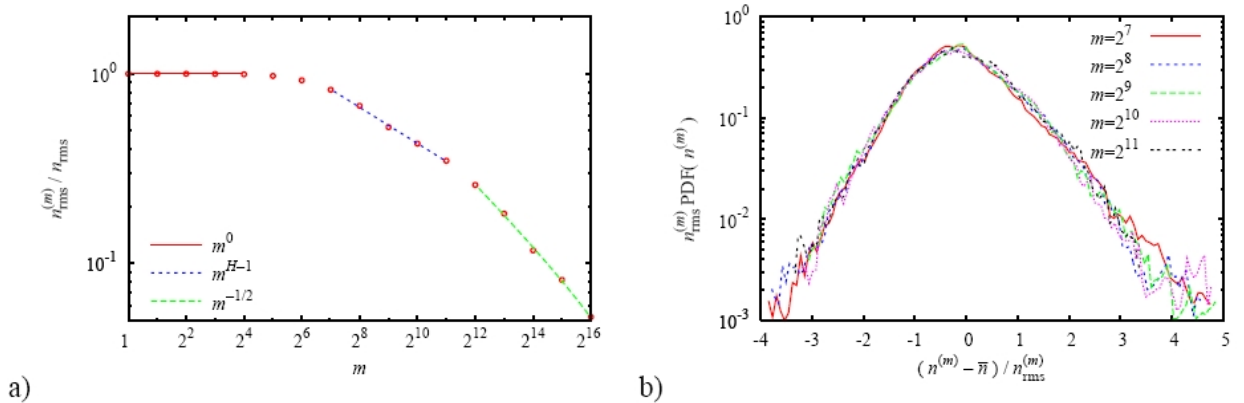


FIG. 5: a) Scaling of the standard deviation  $n_{\text{rms}}^{(m)}$  of the coarse grained particle density fluctuations recorded on probe  $P_3$ . The self-similarity parameter  $H = 0.68$ . b) Rescaled PDF s of the coarse grained particle density fluctuations  $n^{(m)}$  recorded at probe  $P_3$  for the self-similarity range  $128 \leq m \leq 2048$ .

The latter indicates the high probability of large fluctuations corresponding to the presence of blobs of excess plasma as compared to the ambient SOL parameters. The strong increase of particularly the flatness far into the SOL indicates that the structures with largest amplitudes propagate further out in the SOL than the smaller ones.

In Figure 4b we present the rescaled PDF s of the particle density signals taken from a long-run simulation containing several hundred global burst events. For each probe position

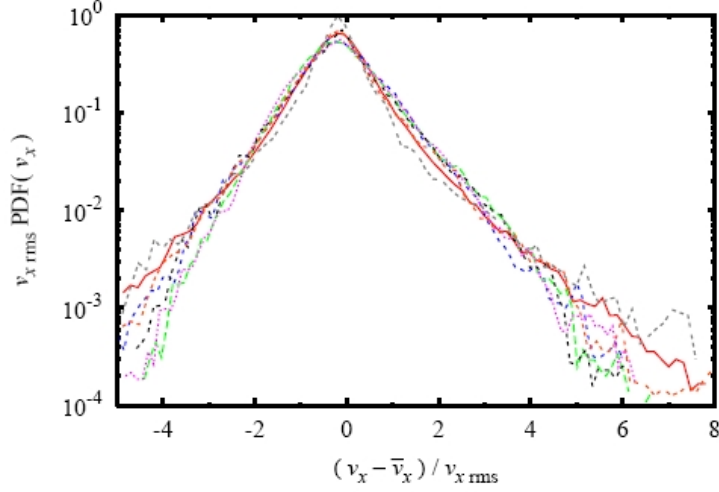


FIG. 6: Rescaled PDF of the turbulent  $E \times B$  velocity recorded at probes  $P_1 - P_7$ .

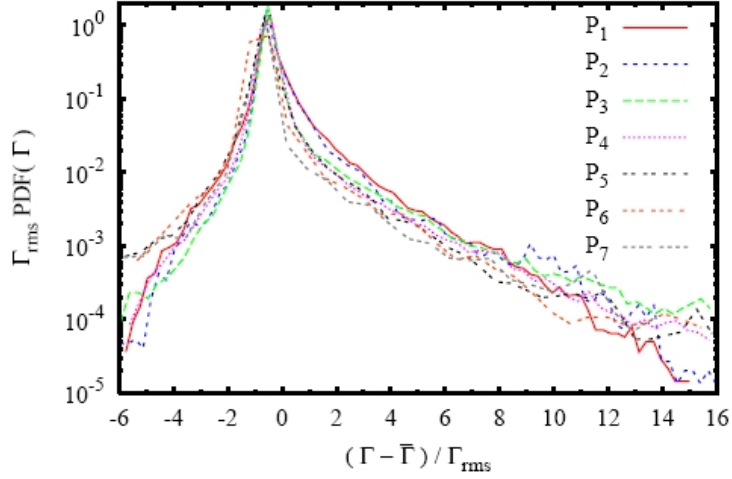


FIG. 7: Rescaled PDF s of the radial turbulent particle flux  $\Gamma$  measured by the different probes  $P_i$ .

the signal is shifted with respect to its local average value  $\bar{n}$ , normalized with the standard deviation  $n_{\text{rms}}$ , and the PDF is scaled with  $n_{\text{rms}}$ . As indicated by the moments presented in Fig. 4a, the particle density fluctuations are normal distributed just inside the LCFS. However, in the SOL the distributions are strongly skewed and flat, exhibiting an exponential tail towards large values. It is noticeable that events with amplitudes as large as eight times the standard deviation is measured. Moreover, for the SOL region the rescaled PDF s all fall on top of each other, showing that there is a statistical similarity of the particle density fluctuations at different radial positions in the SOL. These results are in excellent agreement with experimental

measurements.<sup>18–21</sup>

We have further investigated if the particle density fluctuations have long-range correlations as has been previously demonstrated for various experimental configurations.<sup>41</sup> For this purpose we consider coarse grained particle density signals which are obtained by averaging the original signal with a sampling time of 2.5 in non-dimensional units over adjoining segments of  $m$  points, for details see Ref. 30. For each value of  $m$  we obtain a coarse grained time series denoted  $n^{(m)}$ . A particle density signal possessing long-range correlations over a range of temporal scales will have a self-similar functional form of the rescaled PDF s with power law scaling of the moments with respect to  $m$ . In Fig. 5a we present the variation of the standard deviation  $n_{\text{rms}}^{(m)}$  for the particle density recorded at probe  $P_3$ . Three different scaling regions are identified. First, for values of  $m < 64$ , corresponding to temporal scales  $\tau_m < 160$ ,  $n_{\text{rms}}^{(m)}$  is roughly constant with respect to  $m$ . This is the expected scaling from averaging over temporal scales up to the correlations time, which is roughly at the end of this regime. Second, for scales longer than the correlation time the standard deviation is expected to decrease with increasing  $m$ , and may be expressed as  $n_{\text{rms}}^{(m)} \sim m^{H-1}$ , where we have introduced the self-similarity parameter  $H$ . Note that  $H = 1$  as observed on the fluctuation range corresponds to a deterministic signal, while  $H = 0.5$  is characteristic for uncorrelated random noise. For the intermediate values of  $128 < m < 2048$  we observe a well-defined scaling with  $H = 0.68$ , which indicate long range dependency and self-similarity in the density signal within this regime. The rescaled PDF s of the coarse grained time series presented in Fig. 5b all collapse to the same curve, confirming self-similarity of the particle density signal. The temporal scale corresponding to the upper limit of this similarity range is  $10^4$  in non-dimensional units, and corresponds to the time of the bursting in the global fluctuation level, confer Fig. 2. Coarse graining the signal over larger temporal scales effectively smoothes out these large events, and we may readily expect that normal statistics is approached. Indeed, for larger values of  $m$  the self-similarity parameter  $H$  is close to 0.5. This latter transition could also be influenced by the finite length of our time series.

The large amplitude blob structures in the particle density will result in strong bursts of the local radial turbulent particle flux, which is obtained as  $\Gamma = m v_x$  where  $v_x = -\partial\phi/\partial y$  is the radial component of the fluctuating  $E \times B$  velocity. In Fig. 6 we show the PDF s of the radial velocity component obtained from at the different probes  $P_i$  shown in Fig. 1. The PDF s at the different positions are rescaled with respect to the local time average value  $\bar{v}_x$  and standard deviation  $v_{x\text{rms}}$ . It is noteworthy that the PDF s show an almost similar shape for all probe positions both inside and outside the LCFS in contrast to the density fluctuations. The PDF s are

skewed to the positive side and have broad tails with exponential fall off. The PDF s of the local particle flux  $\Gamma$ , measured at the different probe positions, are presented in Fig. 7. The PDF s are rescaled with respect to the local time average value  $\bar{\Gamma}$  and standard deviation  $\Gamma_{\text{rms}}$ . The PDF s are strongly skewed in the positive direction and characterized by having a sharp peak at low values as well as a broad tail with a roughly exponential shape, reflecting the bursty nature of the local flux time series dominated by large events with deviations from the mean of more than fifteen times the standard deviation. Moreover, as for the velocity fluctuations there is a striking similarity of the rescaled flux PDF s at all radial positions, inside as well as outside the LCFS. Similar observations have been reported for the turbulent particle flux measured in the edge and SOL plasma in tokamak as well as in stellarator configurations.<sup>42</sup>

As we have discussed in connection with Fig. 2 the turbulence has a quasi-periodic bursting behaviour. The typical period is related to the viscous dissipation rate of the sheared poloidal flow. The bursts in the particle flux are naturally related to the turbulent bursts. We can obtain a measure for the repetition rate of the large bursts in the flux from the waiting time statistics for conditional flux events. In Fig. 8 we depict the histogram of waiting times,  $\Delta t$ , between successive events in the poloidally averaged radial flux,  $\Gamma_0$  subject to the condition  $\Gamma_0 - \bar{\Gamma}_0 > 4\Gamma_{0\text{rms}}$ . We observe a clear peak at a waiting time of  $10^4$ , corresponding to the averaged period observed of the turbulent bursts, Fig. 2. The histogram of waiting times has a pronounced tail towards larger times resulting in an averaged value of  $2 \times 10^4$ . Similar waiting time statistics for density fluctuations have also been observed experimentally, see, e.g., Ref. 18.

From the observations above, revealing that the transport is dominated by large bursts, it appears evident that it will not be possible to describe the transport in the SOL by a simple diffusion process combined with a convective flux. Such a parametrization is often used in transport models, see e.g. Ref. 43, that is the flux is expressed as:

$$\Gamma = nV_{\text{eff}} - D_{\text{eff}} \frac{\partial n}{\partial x}, \quad (5)$$

where  $D_{\text{eff}}$  is the effective diffusion coefficient and  $V_{\text{eff}}$  is an effective convection velocity. Writing Eq. (5) in the form:<sup>2,15</sup>

$$\frac{\Gamma}{n} = V_{\text{eff}} - D_{\text{eff}} \frac{1}{n} \frac{\partial n}{\partial x}, \quad (6)$$

we observe that a meaningful parametrization of the flux in the form in Eq. (5) would imply a linear relationship between  $\Gamma/n$  and  $\partial \log n / \partial x$  from which  $D_{\text{eff}}$  is obtained as the slope and  $V_{\text{eff}}$  as the intersection of the line with the vertical axis. In Fig. 9 we have plotted the variation of  $\Gamma/n$  versus  $\partial \log n / \partial x$  for the ESEL simulations. It is clearly observed that the parametrization

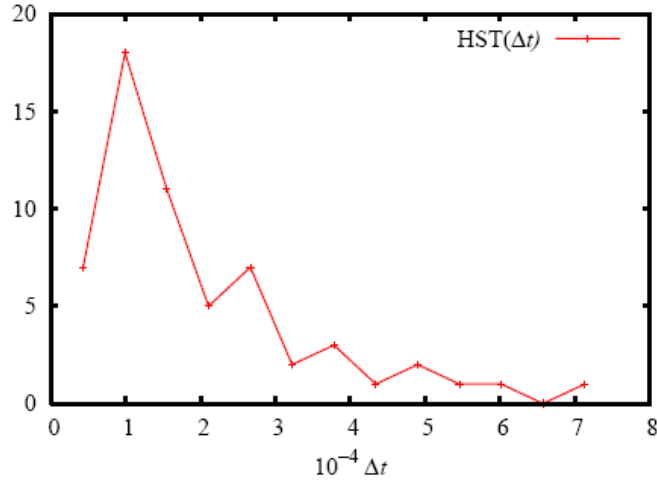


FIG. 8: Histogram of waiting times for the burst events in the radial particle flux measured at probe *P3*.

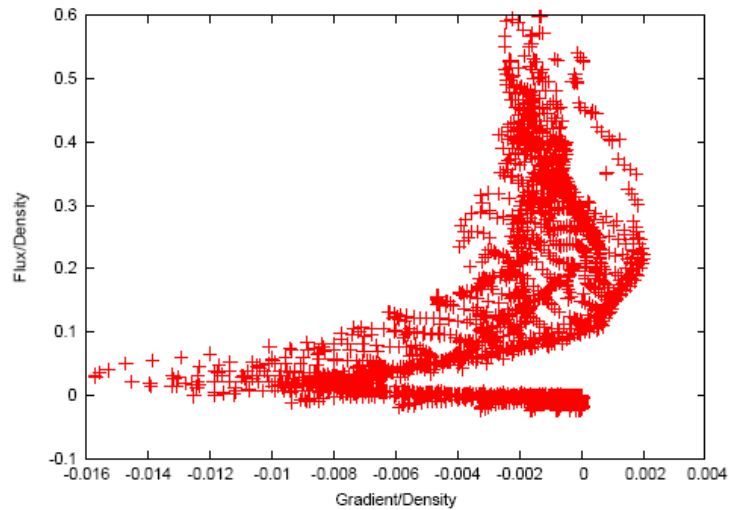


FIG. 9: Scatter plot of the particle flux versus the density gradient.

Eq. (5) really makes no sense, the points are scattered without any functional relationship. Similar observations are found from measured and ESEL simulated fluxes for the TCV tokamak<sup>32</sup> for a range of plasma densities. Thus, at least for these cases a simple parametrization is out of reach. This implies that the full flux PDF has to be known for predictions of the plasma transport in the SOL and in particular for predicting power loads on the plasma facing components, which is an issue of highest concern in the construction of large scale fusion experiments and ultimately fusion power plants.

#### IV. MIXING AND TRANSPORT OF PASSIVE TRACERS

In the previous section we have demonstrated that the turbulent particle flux in the SOL is strongly intermittent in time as well as space. It is of interest to investigate how this intermittency will influence the transport and spreading of impurity ions that are released locally in space. In particular, impurities may originate from the plasma facing components far out in the SOL, and it is of importance to investigate, how they are transported into the core plasma. We shall here present initial studies of the impurity transport in the SOL as governed by the interchange turbulence described in the previous section. The dynamics of impurities is modelled by means of the passive tracer particle approach, assuming that the impurity particle density is much lower than the plasma particle density.<sup>15,17</sup> We thus follow tracer particles that are passively advected by the inherent turbulent motions, but do not back-react on the turbulence. The trajectories of tracers are calculated by integrating their equation of motion,

$$\frac{d\mathbf{x}}{dt} = \frac{1}{B(x)} \hat{\mathbf{z}} \times \nabla\phi, \quad (7)$$

where the tracer velocity is taken to be the electric drift. Thus, we have neglected the effect of finite inertia on the tracer dynamics and limit ourself to tracer ions having a mass to charge ratio smaller than or similar to that of the plasma ions. Note that the  $E \times B$ -drift is compressible due to the spatial dependence of the magnetic field. Including finite inertia effects will add additional compressibility to the convective velocity, which may lead to clustering of particles.<sup>16</sup>

We have employed a bi-cubic interpolation scheme to provide the velocity at the exact particle position, which is usually not at the grid nodes. This method uses the values of the dependent variables and their derivatives at the grid nodes forming the corners of the rectangle that encloses the particle. The derivatives at the particle position are found by using a spectral scheme.<sup>14</sup> A large number of tracers, typically of the order  $10^6$ , have been followed, they were either released uniformly over space or locally in the radial direction along a poloidal stripe. In Fig. 10 we show the evolution of the radial coordinate of a typical trajectory for a tracer released inside the LCFS during a quiet period. The tracer is randomly oscillating inside the LCFS until it is captured by a structure and perform a long flight to the far SOL. However, the tracer is subsequently transported back into the edge region. Long flights may be found both in the radially outgoing and ingoing directions.

Correspondingly, the PDF of the radial step size is strongly non-Gaussian, see Fig. 11, where we show the PDF of the radial step size,  $\Delta x$ , measured over a time interval of  $\Delta t = 50$  and

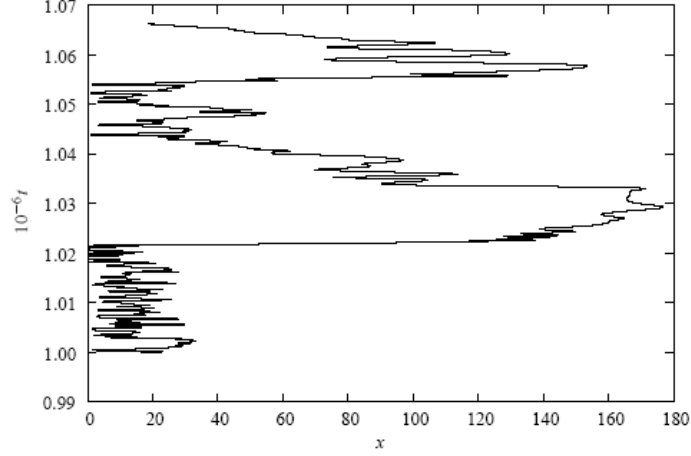


FIG. 10: Typical evolution of the radial position of an impurity particle released in the plasma edge region.

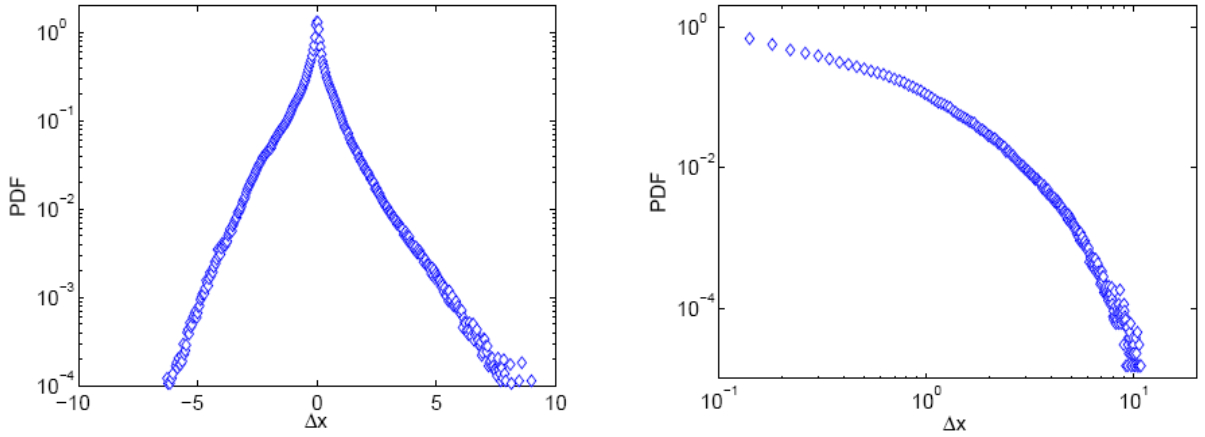


FIG. 11: The PDF of the radial displacement,  $\Delta x$ , measured over  $\Delta t = 50$  of all particles (left panel). The tail in log-log plot. (right panel).

averaged over all particles. The mean value of  $\Delta x$  is close to zero ( $\langle \Delta x \rangle = -0.08$ ), and the standard deviation,  $\sigma = 1.02$ . The PDF is slightly skewed with a positive skewness,  $S = 0.4$ , and has a kurtosis,  $K = 10.7$ , signifying broad tails, which are observed to be exponentially decaying (see right panel of Fig. 11). The tails are near symmetric, i.e., long steps are almost equally probable in both in- and outgoing directions. The step size PDF is found to be self-similar with respect to the time interval  $\Delta t$ , this is quantified in Fig. 12. Here we show the PDF's for the radial velocity component,  $V_x = \Delta x / \Delta t$ , of particles released inside the LCFS (at

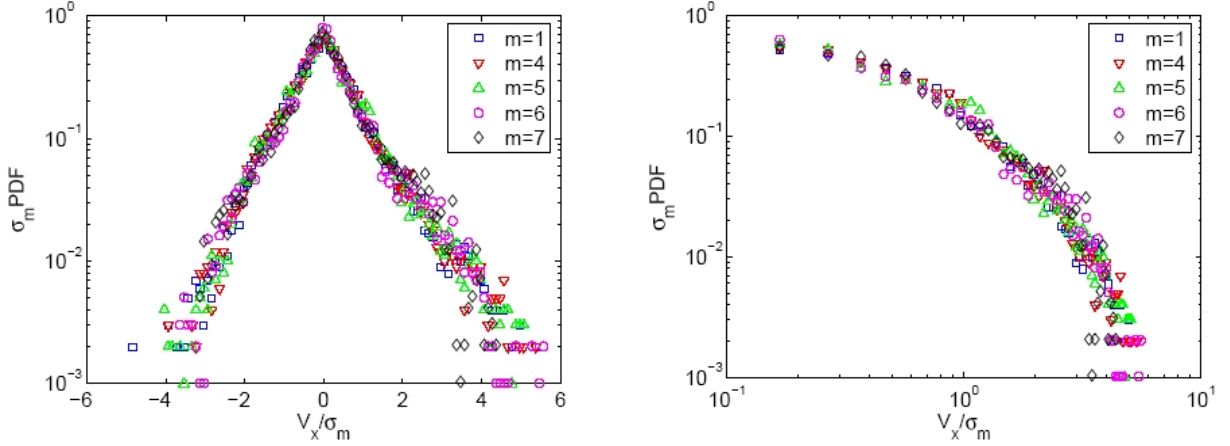


FIG. 12: The re-scaled PDF of the radial particle velocity coarse grained over time intervals  $\Delta t = 50 \times 2^{m-1}$  for particles released inside the LCFS (left panel). The tail in log-log plot (right panel).

$x = L_x/12$ ) for increasing values of  $\Delta t$ . The PDF's are re-scaled as  $\sigma_m \text{PDF}(V_x/\sigma_m)$ , where  $\sigma_m$  is the standard deviation of the coarse grained velocity fluctuations, and they are observed to fall into coincidence. These PDF's are hardly distinguishable from the PDF's obtained by averaging over particles released uniformly in the whole domain. Furthermore, the particle velocity PDF is comparable to the re-scaled PDF of the electric drift velocity, which have the same functional form throughout the whole simulation domain, see Fig. 6.

We should stress here that although we find broad tails on the radial displacement PDF's, the fall off at large values is always observed to be near exponential and cannot be described as a power law which may signify Levy-type statistics. In that connection we should mention the investigations by del-Castillo-Negrete *et al.*<sup>44</sup> of particle dispersion in a somewhat similar setting; a model for resistive pressure gradient driven plasma turbulence. They find clear evidence for (Levy-type) statistics with algebraically decaying particle displacement PDF's for particles released locally in the radial direction. Their observations are well described by a transport model with fractional derivatives both in space and time (see, e.g., Ref. 45–47 for a discussion of fractal diffusion equations). As stated above we have observed no clear evidence for such a behaviour, maybe because our system is spatially restricted in the radial direction and the turbulence is inhomogeneous, with the result that the turbulence amplitude decay when approaching the outer boundary. This will thus preclude the long flights when approaching the outer boundary. These effects are subject of ongoing investigations.

Here we are interested in monitoring the spreading and mixing efficiency of the particles

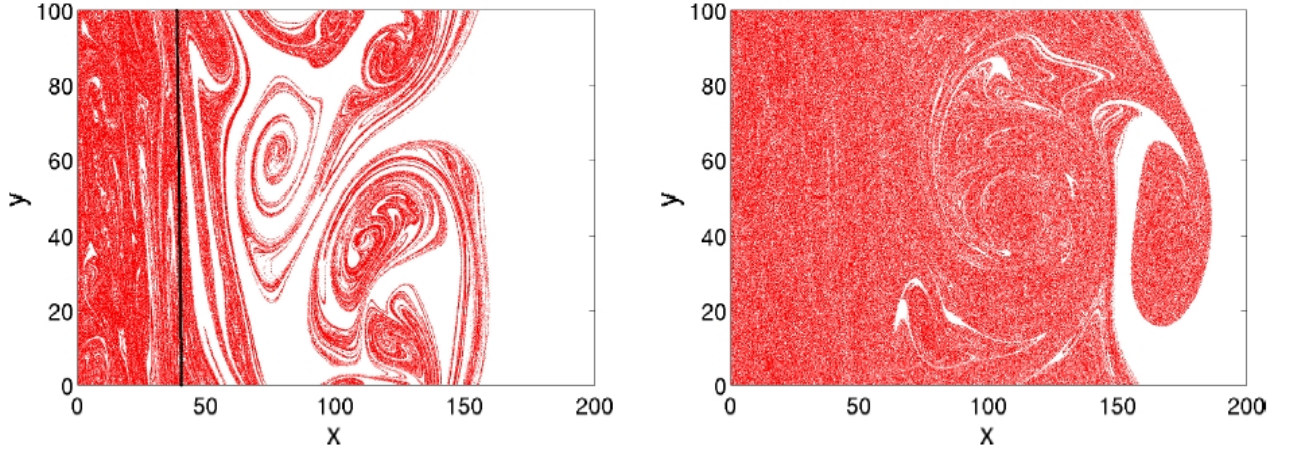


FIG. 13: The mixing of particles initially released in a narrow band just inside LCFS  $39 < x < 41$ , indicated by the black vertical line. Left panel shows particle distribution at  $t = 10.000$  and right panel shows the distribution at  $t = 25.000$ .

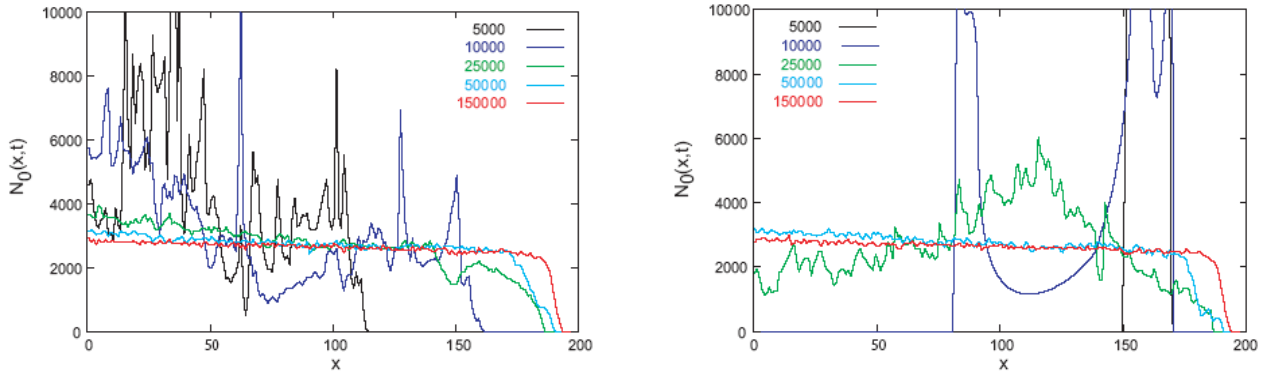


FIG. 14: Evolution of the impurity density  $N_0$  averaged over the  $y$ -direction. Impurities are released in a narrow band; around  $x = 40$  (left panel) and  $x = 160$  (right panel).

all over the SOL. We have thus released the particles in a poloidal band with a narrow radial extension.

In Fig. 13 we show the distribution of the particles originally placed in a band  $39 \leq x \leq 41$  just inside the LCFS. It is observed that the particles spread very fast into the SOL within a time corresponding to the quasi period of the burst and after  $t = 25000$  they are uniformly distributed over the SOL. This is quantified further in Fig. 14 where we present the evolution of the impurity density,  $N_0$ , averaged over the poloidal  $y$ -direction for the cases where the impurities are released inside the LCFS (left panel) and far into the SOL (right panel). The particles are

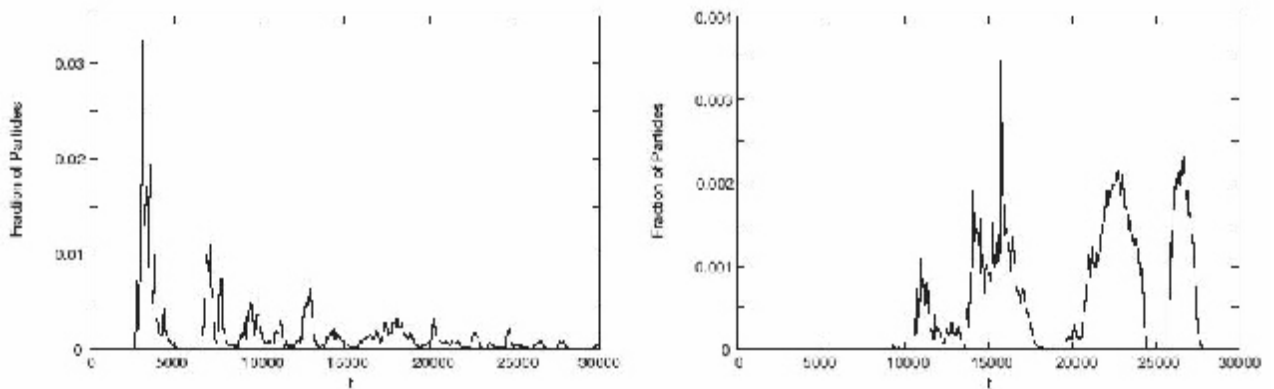


FIG. 15: The relative number of particles on their first passing through a radial plane at  $x = 80$  (left panel) and at  $x = 160$  (right panel) versus time for particles released inside LCFS  $39 < x < 41$ .

rapidly mixed and after a time of the order of  $\tau_{\text{burst}}$ , the particles released inside LCFS already penetrate far into the SOL. The velocity of the front of the particles is larger than 0.02, which is around the typical blob speed, see Sec. III. The particles released in the SOL are mixing at a slower rate, but after a time of only a couple of burst periods they penetrate inside the LCFS. Ultimately the impurity density profile ends up following the same functional shape as the inhomogeneous magnetic field. This final profile is independent of where the particles are released. The transport is certainly not governed by a standard ‘‘Fickian’’ diffusive process. It can be described by an effective pinch, which may be understood by considering the continuity equation for the impurity particle density  $N^{15,48}$ ,

$$\left( \frac{\partial}{\partial t} + \frac{1}{B} \hat{\mathbf{z}} \times \nabla \phi \cdot \nabla \right) \frac{N}{B} = 0,$$

implying that  $N/B$  is a Lagrangian invariant advected by the compressible electric drift  $\hat{\mathbf{z}} \times \nabla \phi / B$ . Now, assuming that the impurities are effectively mixed by the turbulent velocity fluctuations, this invariant will be uniformly distributed in space and the poloidally averaged impurity density  $N_0(x)$  varies like  $B(x)$ . Thus, impurities are effectively mixed within a few burst periods and even if originating far out in the SOL they will quickly penetrate across the LCFS into the edge plasma. This corresponds to the so-called inward (curvature) pinch.

Finally, we have investigated the arrival time statistics. In Fig. 15 we show the relative number of particles passing through two poloidal planes at  $x = 80$  (left panel) and  $x = 160$  (right panel), respectively versus time. Only the first passage is counted. We observe that the particles arrives in clumps indicating that they are transported intermittently by the blob structures. The

arrival of the first particles corresponds to a velocity of 0.02. Note that after  $T = 30000$  less than 25% of the particles have passed the plane at 160.

## V. CONCLUSIONS

We have discussed the basic statistical features of the turbulence and the associated transport in a two-dimensional model for interchange dynamics and demonstrated that it provides results in good agreement with that reported from experimental investigations of SOL turbulence and transient transport events.<sup>18–22</sup> A salient feature of our model is the spatial separation between linear forcing and damping regions. The results agree with the prevailing paradigm of field-aligned blob-like structures generated close to the LCFS and propagating far into the SOL. The associated intermittent transport may have severe consequences for magnetic confinement experiments by producing large localized heat loads on plasma facing components.

The statistical properties of the particle density fluctuations reveal spatial similarity in the sense that the rescaled PDFs have the same functional shape throughout the SOL with an exponential tail towards fluctuations as large as eight times the local standard deviation. Additionally, from coarse graining the time series it is demonstrated that the particle density fluctuations are self-similar, possessing long range dependence over temporal scales from the correlation time to the times associated with the bursting in the global fluctuation level. Similar properties of the particle density fluctuations has recently been demonstrated in various experimental investigations.

Also the PDFs of the turbulent radial particle flux have a spatial self-similar form which seems to extend over the whole plasma boundary region, comprising the edge plasma as well as the SOL. The strongly anomalous statistics of fluctuations and transport at the boundary of confined plasmas underlines the need for a statistical treatment rather than the traditional modeling approach based on the computation of effective transport coefficients. Statistical similarity of the fluctuating quantities, such as that indicated by the present turbulence simulations, thus suggests a statistical modeling in terms of a universal distribution of the turbulent fluxes.<sup>6,42</sup>

By investigating the dynamics of passive tracers modelling impurity species we observed a fast mixing in the SOL and across the LCFS. In spite of the intermittent turbulent transport in the SOL, the passive particles are uniformly mixed within a short time scale. The passive tracers furthermore showed a pinch-like transport mitigated by the compressibility of the electric drift due to the inhomogeneous magnetic field. Tracers initialized far out in the SOL penetrate into

the edge plasma within few bursts periods. It is emphasized that the impurity dynamics cannot be described by a simple diffusion approach.

### Acknowledgement

This paper is dedicated to the memory of Professor Radu Balescu for his pioneering contributions to the understanding of anomalous transport in magnetized plasmas. The work was supported by the Danish Agency for Science, Technology and Innovations (FNU grant 272 06 0367) and the Danish Center for Scientific Computing through grant nos. CPU-1101-08 and CPU-1002-17. O. E. Garcia has been supported by financial subvention from the Research Council of Norway and from Danish Agency for Science, Technology and Innovations. Discussions with W. Fundamenski, J. Graves, O. Grulke, R. Pitts and K. Rypdal are gratefully acknowledged. Furthermore, we thank J. Gavnholt and S. Boudaud for their contributions to the tracer particle investigations.

- 
- <sup>1</sup> S. J. Zweben, J. A. Boedo, O. Grulke *et al.*, Plasma Phys. Controlled Fusion **49**, S1.
  - <sup>2</sup> V.Naulin, J. Nucl. Mater. **363-365**, 24-31 (2007).
  - <sup>3</sup> R. Balescu, *Aspects of Anomalous Transport in Plasmas*, Taylor and Francis Group, CRC Press 2005.
  - <sup>4</sup> T. Huld, A. H. Nielsen, H. L. Pécseli, and J. Juul Rasmussen, Phys. Fluids B **3**, 1609 (1991);  
A. H. Nielsen, H. L. Pécseli, and J. Juul Rasmussen, Phys. Plasmas **3**, 1530 (1996).
  - <sup>5</sup> B.A. Carreras, C. Hidalgo, E. Sánchez, M. A. Pedrosa, R. Balbín, I. García-Cortés, B. P. van Milligen, D. E. Newman, and V.E. Lynch, Phys. Plasmas **3**, (1996) 2664–2672.
  - <sup>6</sup> V. Naulin, O. E. Garcia, A. H. Nielsen, and J. J. Rasmussen, Phys. Lett. A **321**, 355 (2004).
  - <sup>7</sup> G. I. Taylor, Proc. Lond. Math. Soc. **20** 196 (1922).
  - <sup>8</sup> W.D. McComb, *The Physics of Fluid Turbulence* (Clarendon Press, Oxford, 1990).
  - <sup>9</sup> J. H. Misguich, R. Balescu H.L. Pécseli, T. Mikkelsen, S.E. Larsen, and Qui Xiaiming, Plasma Phys. Controlled Fusion **29**, 825 (1987).
  - <sup>10</sup> M. Pettini, A. Vulpiani, J. H. Misguich, M. D. Leener, J. Orban, and R. Balescu, Phys. Rev. A **38**, 344 (1988).
  - <sup>11</sup> M. Vlad, F. Spineanu, J. H. Misguich, and R. Balescu, Phys. Rev. E **58**, 7359 (1998).
  - <sup>12</sup> J.-D. Reuss and J. H. Misguich, Phys. Rev. E **54** (1996) 1857–1869.

- <sup>13</sup> V. Naulin, A.H. Nielsen, and J. Juul Rasmussen, *Phys. Plasmas* **6**, 4575 (1999).
- <sup>14</sup> R. Basu, Th. Jessen, V. Naulin, and J. Juul Rasmussen, *Phys. Plasmas* **10**, 2696 (2003); R. Basu, V. Naulin, and J. Juul Rasmussen, *Comm. Nonlinear Sci. and Numerical Sim.* **8**, 477 (2003).
- <sup>15</sup> V. Naulin, *Phys. Rev. E* **71**, 015402R (2005);
- <sup>16</sup> M. Priego, O. E. Garcia, V. Naulin, and J. J. Rasmussen, *Phys. Plasmas* **12**, 062312 (2005).
- <sup>17</sup> V. Naulin, O. E. Garcia, M. Priego, and J. Juul Rasmussen, *Physica Scripta* **T 122**, 129, (2006)
- <sup>18</sup> G. Y. Antar, *Phys. Plasmas* **10**, 3629 (2003).
- <sup>19</sup> G. Y. Antar, S. I. Krashennnikov, P. Devynck, R. P. Doerner, E. M. Hollmann, J. A. Boedo, S. C. Luckhardt, and R. W. Conn, *Phys. Rev. Lett.* **87**, 065001 (2001); G. Y. Antar, P. Devynck, X. Garbet, and S. C. Luckhardt, *Phys. Plasmas* **8**, 1612 (2001). G. Y. Antar, G. Counsell, Y. Yu, B. LaBombard, and P. Devynck, *ibid.* **10**, 419 (2003).
- <sup>20</sup> J. A. Boedo, D. Rudakov, R. Moyer *et al.*, *Phys. Plasmas* **8**, 4826 (2001); J. A. Boedo, D. L. Rudakov, R. A. Moyer *et al.*, *ibid.* **10**, 1670 (2003); J. A. Boedo, D. L. Rudakov, R. J. Colchin *et al.*, *J. Nucl. Mater.* **313–316**, 813 (2003); D. Rudakov, J. A. Boedo, R. A. Moyer *et al.*, *Plasma Phys. Controlled Fusion* **44**, 717 (2002).
- <sup>21</sup> M. Endler, H. Niedermeyer, L. Giannone, E. Holzhauser, A. Rudyj, G. Theimer, N. Tsois, and the ASDEX Team, *Nucl. Fusion* **35**, 1307 (1995); E. Sánchez, C. Hidalgo, D. López-Bruna *et al.*, *Phys. Plasmas* **7**, 1408 (2000); G. S. Kirnev, V. P. Budaev, S. A. Grashin, E. V. Gerasimov, and L. N. Khimchenko, *Plasma Phys. Controlled Fusion* **46**, 621 (2004); J. P. Graves, J. Horacek, R. A. Pitts, and K. I. Hopcraft, *ibid.* **47**, L1 (2005).
- <sup>22</sup> J. L. Terry, S. J. Zweben, K. Hallatschek *et al.*, *Phys. Plasmas* **10**, 1739 (2003); S. J. Zweben, D. P. Stotler, J. L. Terry *et al.*, *Phys. Plasmas* **9**, 1981 (2002); S. J. Zweben, R. J. Maqueda, D. P. Stotler *et al.*, *Nucl. Fusion* **44**, 134 (2004). O. Grulke, J. L. Terry, B. LaBombard, and S. J. Zweben, *Phys. Plasmas* **13** (2006); S. J. Zweben, R. J. Maqueda, J. L. Terry *et al.*, *Phys. Plasmas* **13**, 056114 (2006).
- <sup>23</sup> S. I. Krashninnikov, *Phys. Lett. A* **283**, 368 (2001); D. A. D’Ippolito, J. R. Myra, and S. I. Krashninnikov, *Phys. Plasmas* **9**, 222 (2002); N. Bian, S. Benkadda, J.-V. Paulsen, and O. E. Garcia, *ibid.* **10**, 671 (2003); D. A. D’Ippolito, J. R. Myra, S. I. Krashninnikov, G. Q. Yu, and A. Y. Pigarov, *Contrib. Plasma Phys.* **44**, 205 (2004).
- <sup>24</sup> O. E. Garcia, N. H. Bian, V. Naulin, A. H. Nielsen, and J. Juul Rasmussen, *Phys. Plasmas* **12**, 090701 (2005); O. E. Garcia, N. H. Bian, and W. Fundamenski, *Phys. Plasmas* **13**, 082309 (2006).

- <sup>25</sup> A. Kirk, H. R. Wilson, G. F. Counsell *et al.*, Phys. Rev. Lett. **92**, 245002 (2004); A. Kirk, H. R. Wilson, R. Akers *et al.*, Plasma Phys. Controlled Fusion **47**, 315 (2005); A. Kirk, N. Ben Ayed, G. Counsell *et al.*, Plasma Phys. Controlled Fusion **48**, B433 (2006).
- <sup>26</sup> B. Gonçalves, C. Hidalgo, M. A. Pedrosa, C. Silva, R. Balbín, K. Erents, M. Hron, A. Loarte, and G. Matthews, Plasma Phys. Controlled Fusion **45**, 1627 (2003); W. Fundamenski, W. Sailer, and JET EFDA contributors, Plasma Phys. Controlled Fusion **46**, 233 (2004); M. Endler, I. García-Cortés, C. Hidalgo, G. F. Matthews, ASDEX Team, and JET Team, Plasma Phys. Controlled Fusion **47**, 219 (2005).
- <sup>27</sup> W. Fundamenski, V. Naulin, T. Neukirch, O. E. Garcia, and J. Juul Rasmussen, Plasma Phys. Controlled Fusion **49**, R43 (2007).
- <sup>28</sup> O. E. Garcia, V. Naulin, A. H. Nielsen, and J. Juul Rasmussen, Phys. Rev. Lett. **92**, 165003 (2004).
- <sup>29</sup> O. E. Garcia, V. Naulin, A. H. Nielsen, and J. Juul Rasmussen, Phys. Plasmas, **12**, 062309 (2005).
- <sup>30</sup> O. E. Garcia, V. Naulin, A. H. Nielsen, and J. Juul Rasmussen, Physica Scripta **T122**, 89 (2006).
- <sup>31</sup> O. E. Garcia, J. Horacek, R. Pitts, A. H. Nielsen, W. Fundamenski, J.P. Graves, V. Naulin, and J. Juul Rasmussen, Plasma Phys. Controlled Fusion **48**, L1 (2006).
- <sup>32</sup> O. E. Garcia, R. A. Pitts, J. Horacek, A. H. Nielsen, W. Fundamenski, J. P. Graves, V. Naulin and J. Juul Rasmussen, J. Nucl. Mater. **263-265**, 575 (2007).
- <sup>33</sup> O. E. Garcia, J. Horacek, R. A. Pitts, A. H. Nielsen, W. Fundamenski, V. Naulin, and J. Juul Rasmussen, Nucl. Fusion, (2007) **47**, 667 (2007).
- <sup>34</sup> R. A. Pitts, J. Horacek, W. Fundamenski, O. E. Garcia, A. H. Nielsen, M. Wischmeier, V. Naulin and J. Juul Rasmussen, J. Nucl. Mater. **263-265**, 505. (2007).
- <sup>35</sup> W. Fundamenski, O. E. Garcia, V. Naulin, R. Pitts, A. H. Nielsen, J. Juul Rasmussen, J. Horacek, and J.P. Graves and JET EFDA, Nucl. Fusion **47**, 417 (2007).
- <sup>36</sup> V. Naulin, W. Fundamenski, A. H. Nielsen, O. E. Garcia, J. Juul Rasmussen, B. Goncalves, C. Hidalgo, M. Hron et al., Proc. 21th IAEA Fusion Energy Conferenre 2006 (Chengdu, China) Paper TH/P6-22.
- <sup>37</sup> O. E. Garcia, J. Plasma Phys. **81**, 65 (2001); European J. Physics **24**, 331 (2003); E. Tassi, O. E. Garcia, J. V. Paulsen, K. Rypdal, and C. Riccardi, Physica Scripta **T113**, 121 (2004).
- <sup>38</sup> V. Naulin, J. Nycander, and J. Juul Rasmussen, Phys. Rev. Lett. **81**, 4148 (1998); V. Naulin, J. Juul Rasmussen, and J. Nycander, Phys. Plasmas **10**, 1075 (2003); *ibid.* **10**, 3804 (2003).
- <sup>39</sup> O. E. Garcia, N. H. Bian, J.-V. Paulsen, S. Benkadda, and K. Rypdal, Plasma Phys. Controlled Fusion

- 45**, 919 (2003); O. E. Garcia and N. H. Bian, Phys. Rev. E **68**, 047301 (2003); Phys. Plasmas **12**, 014503 (2005); N. H. Bian and O. E. Garcia, *ibid.* **10**, 4696 (2003); *ibid.* **12**, 042307 (2005).
- <sup>40</sup> O. E. Garcia, N. H. Bian, V. Naulin, A. H. Nielsen, and J. Juul Rasmussen, Physica Scripta **T122**, 104 (2006).
- <sup>41</sup> B. A. Carreras, B. van Milligen, C. Hidalgo *et al.*, Phys. Rev. Lett. **83**, 3653 (1999); B. A. Carreras, B. van Milligen, M. A. Pedrosa *et al.*, Phys. Plasmas **5**, 3632 (1998); R. Trasarti-Battistoni, D. Draghi, C. Riccardi, and H. E. Roman, *ibid.* **9**, 3369 (2002); K. Rypdal and S. Ratynskaya, *ibid.* **10**, 2686 (2003).
- <sup>42</sup> C. Hidalgo, B. Gonçalves, M. A. Pedrosa *et al.*, Plasma Phys. Controlled Fusion **44**, 1557 (2002); B. Ph. van Milligen, R. Sánchez, B. A. Carreras *et al.*, Phys. Plasmas **12**, 052507 (2005).
- <sup>43</sup> R. Schneider, X. Bonnin, K. Borrass *et al.*, Contrib. Plasma Phys. **46**, 3 (2006).
- <sup>44</sup> D. del-Castillo-Negrete, B. A. Carreras and V. E. Lynch, Phys. Plasmas **11** 3854 (2004).
- <sup>45</sup> R. Balescu, Chaos, Solitons and Fractals **34**, 62 (2007).
- <sup>46</sup> A.V. Milovanov, Phys. Rev. E **63**, 047301 (2001).
- <sup>47</sup> G.M. Zaslavsky, Phys. Rep. **371** 461 (2002).
- <sup>48</sup> M. B. Isichenko and N. V. Petviashvili, Phys. Plasmas **2**, 3650 (1995).